ELSEVIER

Wear 200 (1996) 328–335

WEAR

Generalized effects in confined fluids: new friction map for boundary lubrication

Gustavo Luengo [a], Jacob Israelachvili [a], Steve Granick [b]

[a] *Department of Chemical Engineering, and Materials Department, University of California, Santa Barbara, CA, 93106–5080 USA*

[b] *Department of Materials Science and Engineering, University of Illinois, Urbana, IL 61801, USA*

Abstract

Recent advances in measuring the rheology and tribology of thin liquid films between shearing surfaces have enabled previously-inaccessible parameters to be measured accurately during frictional sliding. These include the real area of contact, the local asperity load and pressure, and the sheared film thickness. The results show striking non-continuum, non-bulk like effects when the thicknesses of sheared films approach molecular dimensions as occurs under most tribological conditions. Based on these new results, we assess the validity of current presentations of friction processes, such as the Stribeck curve, and propose new constitutive relations and a dynamic friction map, including an alternative Stribeck type curve representation, which are also formulated in terms of more accessible parameters.

Keywords: Thin liquid films; Frictional sliding; Rheological behavior; Polymeric fluids

1. Introduction

1.1. Bulk rheological behavior of complex fluids: the WLF equation and related principles of time-temperature and time-pressure superposition.

The use of master curves to represent complex behavior has long been used in many different fields. In the case of complex fluids and polymer systems, the time-temperature superposition principle has allowed the representation of viscoelastic and rheological properties of polymeric fluids, such as the viscosity and the shear moduli, in terms of a master curve using the Williams–Landel–Ferry (WLF) equation [1,2]. With this, the response at a certain point on the frequency or time scale at an initial temperature (or pressure) is changed predictably when this temperature or pressure is altered: the behavior at the new temperature (or pressure) is the same as at the initial one, but shifted predictably on the master curve of response. The WLF equation, however, refers to very gentle deformations.

Long ago, Ludema and Tabor noted the relevance of this equation to the sliding friction of polymers [3]: changes of not only temperature or pressure (as in the original WLF equation), but also of sliding speed simply shift the experimental window of the same master curve to a different part of the same master curve. The WLF representation has been of great practical use to rheologists, in addition to providing theoretical insights because different peaks and valleys in a master curve correspond to a particular molecular relaxation process occurring within the system at that temperature and frequency.

More recently, in sliding situations that did not involve polymers, similar responses have emerged quite independently. The friction force (or rate of energy dissipation) as a function of sliding velocity (or temperature) is found to be bell-shaped. It is low when the velocity is low or high (alternatively, the temperature high or low, respectively) but it passes through a maximum when these variables take intermediate values [4,5]. In confirmation of these findings derived from using the surface forces apparatus, similar conclusions have emerged from FFM (friction force microscopy) [6].

We note parenthetically that the success of master curves in describing tribological response shows that changes of speed and temperature do not involve phase changes. The effect is more subtle than this; the master curve is the same regardless of frequency or sliding speed, but the portion of the master curve sampled by the experiment changes.

2. The Stribeck curve and the three tribological regimes

In contrast, tribologists have generally used the Stribeck curve to represent frictional behavior. The top portion of

PII S0043-1648(96)07248-1

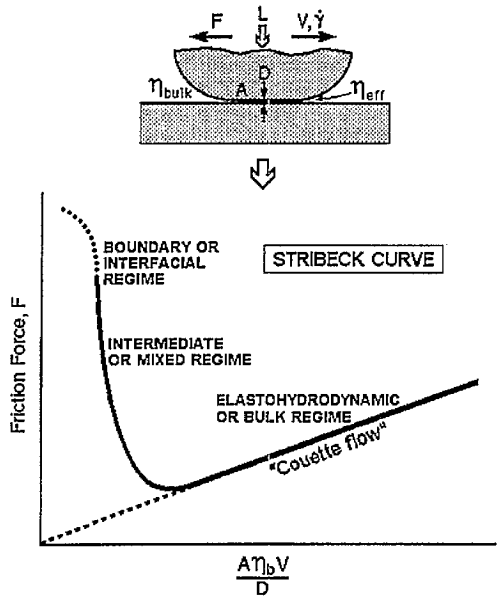

Fig. 1. Traditional Stribeck curve, in which a single curve is considered to describe how the friction force from a lubricant depends on experimental parameters. These parameters are the contact area A, the bulk fluid viscosity η_b, the sliding speed V, and the film thickness D. Note that the last two parameters combine to define the shear rate $\dot{\gamma}=V/D$. With increasing load L, the friction passes from left to right on the Stribeck curve. In reality, the local or microscopic effective viscosity (η_{eff}) may be quite different from the bulk viscosity (η_b).

Fig. 1 contrasts with the macroscopic and microscopic questions at work here. The bulk viscosity, η_b, is the basic ingredient of the multifarious solutions of the Reynolds equation. The microscopic local viscosity between asperities, η_{eff}, is discussed below.

In the traditional scheme supposed by the Stribeck curve, illustrated in Fig. 1, a single curve explains the friction force F or stress $\sigma=F/A$ of a lubricant as a function of the contact area A, the bulk fluid viscosity η_b, the sliding speed V and the film thickness D (the last two parameters combine to define the shear rate $\dot{\gamma}\equiv V/D$). For thick films exhibiting bulk behavior, the frictional drag force F (or shear stress, σ) is given by the classical equation for Couette flow:

$$F=AV\eta_b/D=A\eta_b\dot{\gamma} \quad (1)$$

or

$$\sigma=F/A=V\eta_b/D=\dot{\gamma}\eta_b \quad (2)$$

The Stribeck curve (Fig. 1) is usually described in terms of A, V, D, η_b and the applied load L. This view of lubrication implicitly assumes that changes in V, D and η_b produce effects so similar that they can strictly offset one another.

The presumption that $AV\eta_b/D\equiv A\eta_b\dot{\gamma}$ is the relevant parameter is deficient in several respects. First, these parameters cannot usually be measured during normal tribological processes, so the notion remains rather conceptual and difficult to apply to practical engineering situations. In fact, these parameters (as they refer to local properties) could not generally be measured even with sophisticated laboratory equipment. Second, the presumption, that the product indicated in the abscissa of Fig. 1 is constant, is very strong. For example, it assumes that decreasing the film thickness by one-half has the same effect as doubling the sliding speed. This has never been verified. We focus below on a new approach to describe boundary (or 'interfacial') lubrication.

3. Recent experimental advances

Recent experiments have shown that the bulk fluid viscosity, η_b, does not accurately reflect energy dissipation in ultrathin films. The effective viscosity may be up to seven order of magnitude higher in these films of near-molecular dimensions [7–9]. In addition, discontinuous transitions between different dynamic states (e.g. solid-to-liquid or static-to-kinetic sliding transitions) often occur in thin films, even in these single asperities where issues of mechanical interlocking of opposing solid surfaces cannot come into play [10–16]. The ordering and frictional behavior of the confined molecules are found to switch at some critical load, velocity or temperature (which are different from the melting point of the bulk fluid). Such discontinuous transitions are not considered in the Stribeck curve, nor in the WLF equation.

The aims of our research was to analyze, based on recent experimental data: (1) How far the WLF representation does apply to complex fluids under conditions of extreme confinement as occurs during tribological processes, (2) How to link up, if possible, the WLF representation with the Stribeck curve, and (3) To suggest an improved Stribeck-type curve that is more solidly based on experimental data and that is also formulated in terms of parameters that are easily accessible under engineering (as opposed to laboratory) conditions.

Our motivation for doing this arose from recent experiments on idealized molecularly-smooth surfaces whose real contact area and separation could be directly measured during sliding. Most of this type of research has been done using the Surface Forces Apparatus technique [17] involving independent researchers in different laboratories. In the SFA, the interaction forces between two curved, molecularly smooth surfaces are directly measured. The crossed cylinder geometry is equivalent to two spheres or to a sphere on a flat surface, and thus mimics a single asperity contact. Typical surface radii are $R=0.1-2$ cm and typical contact diameters are 1–100 μm (depending on the applied load).

An optical interference technique is used in which white light is passed through the interacting surfaces in the direction perpendicular to them. The emerging beam is focused onto the slit of a grating spectrometer which splits the beam up into different wavelengths. This produces a series of colored fringes ('FECO fringes' – fringes of equal chromatic order) that provide a means for directly visualizing the surfaces, giving their shape and surface separation (to within 1 Å) and, for surfaces in contact, their exact area of contact (to ±5%). The SFA can be used to measure both normal and

lateral (shear) forces (to ±1%) and pressures (to ±5%), under both static and dynamic conditions, and it is particularly well-suited for studying the structure of and interactions generated by thin liquid films between surfaces.

Such experiments have enabled various tribological, rheological and other dynamic forces to be measured under different conditions of load, sliding velocity, temperature, previous history, etc. and thus allow for a re-evaluation of the parameters that determine F and σ. After reviewing these recent experimental findings, we proceed to consider their application under practical (engineering) conditions, viz., how to express the friction force in terms of readily accessible quantities such as the applied load, sliding velocity, material modulus, ambient temperature, etc., but not the real contact area, film thickness or bulk fluid viscosity. The bulk viscosity may remain valid in the hydrodynamic regime of lubricated sliding (cf. Fig. 1). This is discussed later. However, all of these parameters are directly measurable in a SFA-type experiment, and thus allow us to make this assessment.

4. Experimental observations

4.1. Simple liquids and polymer fluids

SFA experiments have traditionally focused on the forces, viscosity and friction between surfaces across films of common liquids such as water, cyclohexane and liquid paraffins. The molecules of such liquids possess some degree of symmetry, e.g., being spherical or ellipsoidal, or short, linear chains. Such molecules generally exhibit oscillations in their normal force profiles, $F(D)$, which is indicative of molecular ordering, possibly into solid-like layers in films thinner than a few molecular diameters [17]. In sliding experiments, stick-slip motion has been observed [10–16]. Sometimes this has been explained in terms of solid-liquid transitions occurring during sliding: the idea here is that the film is 'frozen' under static (sticking) conditions but is induced to melt (stress-induced melting) when a shear stress is applied, which causes the slip phase.

Recent analysis shows that this presumption is not required when one takes into account the velocity or rate-dependence of stick-slip motion [1–3]. This point we alluded to above in the section concerning the WLF equation, and we now elaborate on it. Experiments by Dhinojwala and Granick [18] show that confined fluids flow smoothly provided the velocity is sufficiently low; they flow by intermittent stick-slip motion only if the rate exceeds the inverse natural relaxation time. This connection between stick-slip and forced motion at a rate that exceeded the inverse natural relaxation time has implications for predicting the onset of stick-slip behavior. The physical interpretation is that when the lubricant is deformed faster than it can keep up, elastic forces built up to the point that catastrophic rupture ('stick-slip') intervenes.

In fact, analogous phenomena are familiar in common experience when a fluid's natural relaxation time falls within the experimental window. Consider, for example, silly putty, honey, or tar. It is a common experience that these fluids flow as liquids if a piece is pulled in opposite directions slowly, but break into two if pulled in opposite directions rapidly. Of course this rate dependence could be described by some postulated relation between force and velocity that would imply instability when the velocity was high [19]; but the description would risk being circular, being based on the postulated assumption. The new point to come from this analysis is the suggestion that the point of unstable motion can be predicted based on knowing the natural relaxation time of the confined fluid film [18].

It is interesting to assess proposed theories of stick-slip in light of these observations. Stick-slip motion has been interpreted to signify that friction decreases with increasing distance traversed or velocity [4,5,19]; however, this assertion does not include a mechanistic interpretation and provides no guide to predict the frequency or shear rate at which the effect will be observed. Another traditional explanation, in terms of the mechanical interlocking of rough surfaces, can be discounted since these atomically-smooth surfaces were separated by water molecules. The more recent view has been that confinement induces crystallization [12–16] or some other phase change [14,15] at rest; discontinuities when motion is forced are attributed to shear melting or some other shear-induced phase transition. However, these experiments showed that the confined films were demonstrably in a fluid state to start with [18]. Only when sheared faster than the natural relaxation time did they display discontinuous motion.

There have also been studies on several polymer melts, such as polydimethylsiloxane (PDMS), polyphenylmethylsiloxane (PPMS), perfluoropolyether (PFPE) and polybutadiene (PBD). In the case of highly asymmetric (irregularly-shaped) molecules, such as branched polymers and those that form glasses rather than crystals in bulk conditions, the normal force profiles are smooth (no oscillations), though stick-slip motion can also be observed. Thus, certain qualitative effects in the dynamic properties are generally observed with all confined fluids regardless of molecular makeup; these include a sharp increase in viscosity and the appearance/development of a finite yield stress.

4.2. The 'effective' viscosity of a lubricating film

For liquids under conditions where they do not show any clear solid-like behavior in thin films (even though they may still exhibit stick-slip motion under certain conditions), shear flow occurs smoothly and — based on Eq. (1) for Couette flow — the measured frictional force F can be described in terms of an 'effective viscosity', defined by

$$\eta_{\text{eff}} = FD/AV \tag{3}$$

here $\eta_{\text{eff}} = \eta_b$ for bulk conditions. Significantly, experiments conducted on a variety of liquids under various conditions of confinement (load, sliding velocity, etc.) have revealed a

roughly inverse relationship between the forces of friction and the bulk viscosity of the liquids, in direct opposition to expectations based on continuum models (cf. Eq. (1)) and the Stribeck Curve (Fig. 1). As previously discussed in the literature [12], the inverse relationship between viscosity and friction forces is caused by the greater tendency of irregularly-shaped molecules, which generally have a higher bulk viscosity, to remain more disordered and liquid-like under confinement, thereby producing a lower resistance to frictional sliding. In all cases, however, the effective viscosities of the confined fluids are significantly higher than the bulk values.

If the degree of branching is slight then this increase is less for irregularly-shaped, such as branched chained molecules, than for spherical or linear chained molecules [12]. But for larger degrees of branching with methyl groups, as (for example) with squalane, then the effective viscosity of the confined lubricant can be extremely large [11], presumably owing to the tendency towards interlocking of opposed irregular structures.

One important exception to these correlations is water, which has been found to exhibit both low viscosity and low friction [13,18]. Since water adsorbs on hydrophillic surfaces, the presence of water can drastically lower the friction, and eliminate the stick-slip of hydrocarbon liquids, when the sliding surfaces are hydrophilic.

There has been much speculation in the literature that the molecular shape of the lubricant could be correlated with tribological properties. More recent work suggests that at tribological pressures (>10–100 MPa) all lubricants studied, regardless of their molecular shape, display stick-slip motion. The reason appears to be explainable by WLF-type arguments: at the rate of the typical tribological experiment, the lubricant acts solid-like because the effective shear rate so far exceeds its inverse natural relaxation time.

Other experiments [7–9] studied the dependence of the effective viscosity of a molecularly thin film on the shear rate. They observed a Newtonian regime ($\eta_{\text{eff}}=$ constant, independent of $\dot{\gamma}$) at low loads and low shear rates, but where η_{eff} is very much higher than the bulk value, η_b. As the shear rate $\dot{\gamma}$ increased, the system reached a point where the effective viscosity started to drop with a power-law dependence on the shear rate (Fig. 2). This shear thinning effect appeared to follow a universal law

$$\eta_{\text{eff}} \propto \gamma^{-n}$$

where

$$\eta_{\text{eff}} \gg \eta_b \tag{4}$$

with n in the range 1/2–1, $n \approx 2/3$ found most commonly. Subsequent theoretical work by a number of authors reproduced this '2/3 power-law', but the scaling models they proposed by way of explanation were not always the same. Urbakh et al. [20] concluded from a physical analysis of lubrication that

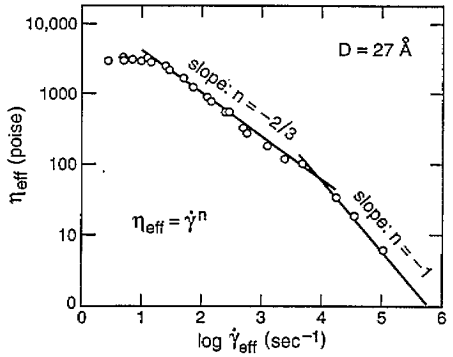

Fig. 2. Example of shear thinning of a simple lubricant when confined to near-molecular dimensions. The effective viscosity decays as a power law, $\eta_{\text{eff}} \propto \dot{\gamma}^{-n}$. In this example (dodecane films of thickness 2.7 nm and net normal pressure 0.12 MPa at 28°C), $n=-2/3$ at low $\dot{\gamma}$ and $n=1$ at high $\dot{\gamma}$ [8]. In the bulk, dodecane is a low-viscosity Newtonian fluid.

$$\eta_{\text{eff}} \propto \gamma^{-n} \tag{5}$$

where n could vary between 2/3 and 1.0, which agrees with the range of exponents found on a number of other different systems, including surfactant monolayers which are not liquid boundary lubricants, discussed below. Rabin and Hersht [21] and Thompson et al. [14] concluded that the '2/3 law' was universal. The computer simulations of Thompson et al. [14,15] on short-chain molecules consisting of 1–24 segments reproduced the power-law scaling behavior, but different exponents were obtained depending on whether the simulations were done at constant pressure ($n=2/3$) or constant film thickness ($n=1/2$). They also obtained a low shear-rate leveling off of the viscosity, as observed in the experiments, which implies a return to Newtonian, but not bulk-like, behavior at very low shear rates.

Recently, Luengo and others have observed a similar power-law behavior in the case of a polymer melt polybutadiene (PBD) [22]. However, by using somewhat different methods than those used by Granick and coworkers they could not access the low shear rate quasi-Newtonian plateau occurring at shear rates below γ_{min}. But the type of system studied (a polymer melt) allowed Luengo and coworkers to observe a leveling off of η_{eff} at the bulk Newtonian value at high shear rates, $\dot{\gamma}_{\text{max}}$, as illustrated in Fig. 3. The critical upper shear rate $\dot{\gamma}_{\text{max}}$ at which the effective viscosity first begins to deviate from the bulk value was found to depend on the film thickness D (which in turn depends on the applied load or pressure) according to, approximately,

$$\dot{\gamma} \propto 1/D \tag{6}$$

5. Proposed friction maps

Based on experiments using different surfaces and systems we can propose the following generalized friction maps. Fig. 4 suggests the proposed behavior of friction force vs. sliding velocity. This figure combines the two effects observed at low and at high shear rates, i.e., the data presented

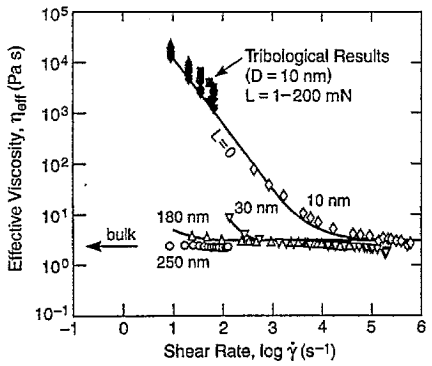

Fig. 3. Effective viscosity plotted against effective shear rate on log-log scales for a polybutadiene (molecular weight 7 000 g $mole^{-1}$) at four different separations, D. Open data points were obtained from sinusoidally-applied shear at zero load ($L=0$) at the indicated separations. Points denoted 'tribological results' were obtained from friction measurements at constant sliding velocities. The tribological results extrapolate, at high shear rate, to the bulk viscosity.

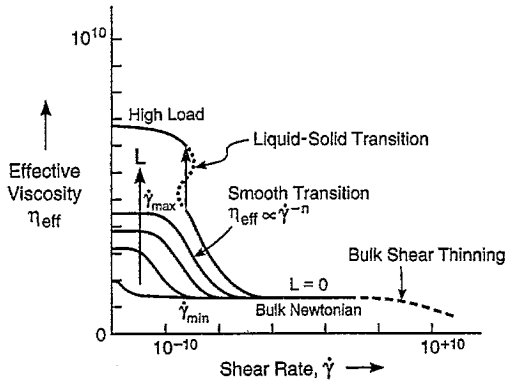

Fig. 4. Proposed generalized friction map of effective viscosity (η_{eff}, arbitrary units) plotted against effective shear rate ($\dot{\gamma}$, arbitrary units) on a log-log scale. We distinguish three main classes of behavior. (1) Thick films; elastohydrodynamic sliding. At zero load ($L=0$), η_{eff} is independent of shear rate except that shear-thinning may be displayed when $\dot{\gamma}$ is sufficiently large. (2) Boundary layer films, intermediate regime. A Newtonian regime is again observed (η_{eff} = constant, independent of $\dot{\gamma}$) at low loads and low shear rates, but η_{eff} is very much higher than the bulk value, η_b. As the shear rate $\dot{\gamma}$ increases beyond γ_{min}, these systems reach a point where the effective viscosity starts to drop with a power-law dependence on the shear rate (cf. Fig. 2), $\eta_{eff} \propto \dot{\gamma}^{-n}$, with n in the range 1/2–1 and $n \approx 2/3$ found most commonly. As the shear rate $\dot{\gamma}$ increases still more, beyond $\dot{\gamma}_{max}$, a second Newtonian plateau is again encountered. (3) Boundary layer films, high load. The η_{eff} continues to grow with load and to be Newtonian provided that the shear rate is sufficiently low. Transition to sliding at high velocity is discontinuous and usually of the stick-slip variety.

in Figs. 2 and 3. At zero load ($L=0$) the system is Newtonian over a very large range of shear rates, with a tendency towards limiting the shear stress behavior occurring at the highest velocities. As the load increases, Newtonian behavior is preserved at low shear rates but the effective viscosity increases above η_b. A second shear thinning mechanism now emerges that connects this enhanced viscosity with the bulk value over a transition regime (non-continuous transitions may also occur, indicated by the vertical arrow in Fig. 4; these are discussed below). In the smooth transition regime the effective viscosity decreases with the general power law given by Eq. (4), where n may vary from below 0.5 to 1.

The smooth transition regime is reminiscent of a similar shear-thinning effect encountered in bulk lubricants at extreme physical conditions, such as high pressure and shear rate, as commonly occurs during elastohydrodynamic lubrication. For these bulk fluids, the non-Newtonian viscosity is empirically described by the Cross equation [23]:

$$\eta(\gamma) = \eta_\infty + [\eta_b - \eta_\infty]/[1 + (\lambda\dot{\gamma})^n] \quad (7)$$

where λ is the Rouse relaxation time of polymer dynamics [2]):

$$\lambda \approx 6\eta_b M/\pi^2 \rho RT \quad (8)$$

which is a measure of the width of the transition spanning the γ axis. Here ρ is the density, R is the gas constant, and T is the absolute temperature. A similar equation may apply in thin films, where Eq. (7) would be replaced by

$$\eta(\gamma) = \eta_{eff} + [\eta_{eff} - \eta_b]/[1 + (\lambda\dot{\gamma})^n] \quad (9)$$

Fig. 5 displays the family of these curves computed for $\gamma = 19.95\ s^{-1}$, $n=1$ and different values of η_{eff}/η_b (as indicated in the figure) chosen to fit the data of Luengo et al. [22]. The agreement appears to be interesting, suggesting that Eq. (9) may serve as a suitable empirical equation for describing the smooth shear-thinning transitions in thin lubricating films. We note that this fit to the generalized Cross equation does not exclude the probability that bulk shear-thinning would occur at still higher shear rates; nor, indeed, the possibility that other thin film transitions could also occur.

From Fig. 4 we also obtain Fig. 6, which relates the friction force F to the sliding velocity V at different loads L. This series of curves, which are now in terms of usually accessible experimental parameters, displays the main features of F-V curves due to the non-linear dependence of F on V and L (note that the load in turn determines the film thickness D and thus the shear rate $\dot{\gamma} = V/D$, as well as the effective viscosity, η_{eff}). Fig. 6 shows that at both high and low velocities the film is Newtonian, but not in-between where dramatic discontinuous changes (vertical and horizontal discontinuities) or WLF-like maxima and minima, may occur (discussed

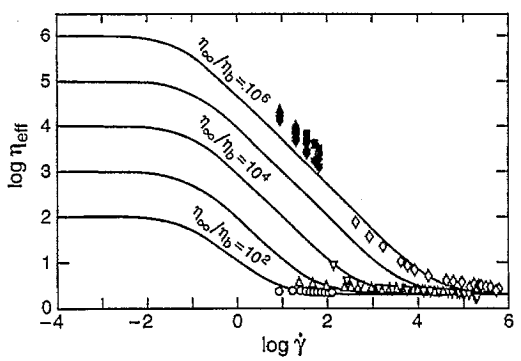

Fig. 5. Fit of data of Luengo et al. [22] to the generalized Cross equation. The effective viscosity of polybutadiene melts is plotted against effective shear rate on log-log scales.

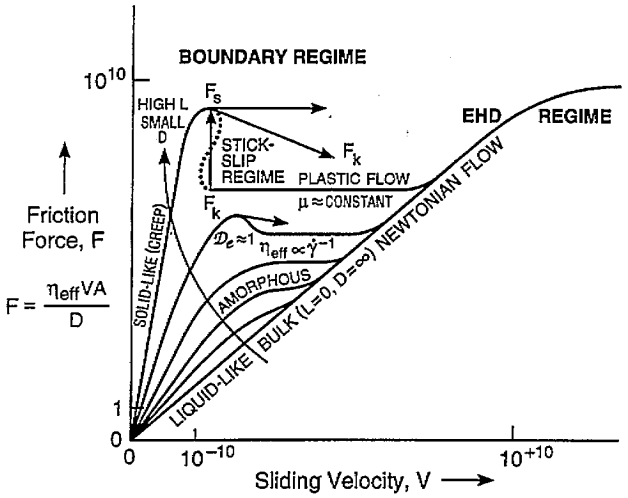

Fig. 6. Proposed friction map of friction force plotted against sliding velocity in various tribological regimes. With increasing load, Newtonian flow in the elasto-hydrodynamic (EHD) regimes crosses into the boundary regime of lubrication. Note that even EHD (elastohydrodynamic) lubrication passes, at the highest velocities, to limiting shear stress response [24–27]. At the highest loads (L) and smallest film thickness (D), the friction force passes a maximum (the static friction, F_s), followed by a regime where the friction coefficient (μ) is roughly constant with increasing velocity (i.e. the kinetic friction, F_K, is roughly constant). Non-Newtonian shear-thinning is observed at somewhat smaller load and larger film thickness; the friction force passes through a maximum at the point where $De \approx 1$ (De, the Deborah number [28], is the point at which the applied shear rate exceeds the natural relaxation time of the boundary layer film). The velocity axis from 10^{-10} to 10^{10} (arbitrary units) indicates a large span. The corresponding F–L map is shown in Fig. 7.

below). It is important to stress, however, that for these interesting non-linear effects to be observed experimentally, the F-axis and especially the V-axis must be varied over a large range.

5.1. Friction maps in thin films

In thin films, the film is no longer bulk-like, but it may still be describable by time-temperature or time-thickness superposition, albeit with modified parameters from the bulk values. The essential importance of rate dependence has been found under mild tribological conditions, not only for confined fluids but also for boundary lubricant films that are not liquids or fluids in the bulk. This should not be surprising: the WLF formalism is well suited to describing highly dissipative systems in general, and so should be expected to describe the dynamic properties of a thin film as it approaches the highly dissipative tribological regime.

The applicability of the WLF formalism to the friction of elastomeric surfaces was demonstrated long ago [3], where it was considered to be an exception that would characterize rubbers only. However, recent friction force experiments in a number of quite different systems have revealed WLF-like bell-shaped $F(T)$ and $F(V)$ curves, also obeying the time-temperature superposition principle, or at least a strong rate-dependence. [1] In the case of confined complex fluids, such as polymer melts, a number of different relaxation processes may be occurring, some of which (for example, those involving chain-surface interactions) will have no bulk counterpart, while those that do may have significantly different relaxation times. A number of peaks and valleys may therefore be expected for such films.

A particularly good example of the applicability of Fig. 4 to a real system is provided by the data in Ref. [29], where shear stress was measured as a function of shear rate for the smectic liquid crystal 8CB (4-cyano-4'-octylbiphenyl). The results revealed non-Newtonian behavior at low shear rates that precisely follows the curves in Fig. 4, including the horizontal instabilities at high stresses.

5.2. Stick-slip motion caused by continuous (WLF-like) and discontinuous (solid-like to liquid-like) transitions

As already mentioned, stick-slip motion can arise when solid-to-liquid transitions occur within a sheared film. At these discontinuous transitions the frictional properties change abruptly. An example of such a transition is shown by the vertical arrow in Fig. 4, whose limits define the static and kinetic friction forces, F_s and F_k.

Fig. 4 shows that stick-slip can also arise from a maximum in the F-V curve (horizontal and sloping arrows). Depending on the system constraints during sliding — whether at constant applied load, shear force or sliding velocity — abrupt jumps will occur from one part of the generalized friction map to another. These instabilities also manifest themselves as stick-slip motion [19,30]. For an elastic system, where the applied shear force may depend on the slip distance moved, a non-horizontal line will define the limits of stick and slip, which in turn define the static and kinetic friction forces, F_s and F_k. A good example of the latter type of transition in a bulk system is provided in Ref. [29] for bulk 8CB.

In transitions determined by a maximum in the F-V curve, the rheological properties of the sheared film, may vary smoothly with the sliding speed or shear rate (WLF-like), rather than changing abruptly between different dynamic phase states. However, to have a maximum in the F-V curve, the effective viscosity in the transition regime of Fig. 4 must fall faster than -1; that is, $n > 1$ in Eq. (4) and Eq. (7). Depending on the magnitude of the negative slope dF/dV, stick-slip motion will result if the stiffness of the system is sufficiently low [19,30].

We propose that the family of curves presented in Fig. 4, Fig. 6 and Fig. 7 offer a much better representation of frictional behavior than the single-curve Stibeck presentation. The curves merge with the WLF description in the bulk limit

[1] It is easy to miss these effects when carrying out experiments over a limited range of velocities, and conclude that Amonton's law of friction, with friction independent of velocity, is obeyed. To fully investigate the velocity-dependence of friction forces one needs to carry out experiments over many decades as the velocity and frequency-dependent effects tend to depend logarithmically rather than linearly on V.

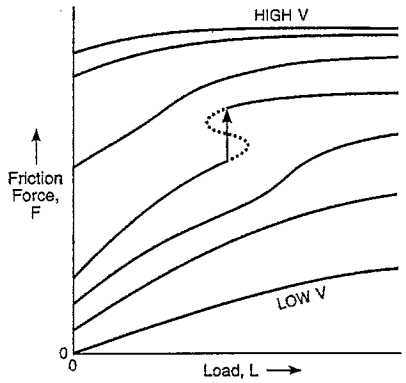

Fig. 7. Proposed friction map of friction force (F) plotted against load in various tribological regimes. With an increasing velocity (V), F increases at first moderately, then more rapidly, with increasing V. A discontinuous transition to F independent of L is eventually expected.

($L=0$), exhibiting bulk-like Couette flow behavior at low loads, but with shear-thinning at high V. As the load increases, there is a transition to a modified WLF-like behavior for low loads and shear rates, changing to abrupt liquid-to-solid like transitions behavior at higher loads. This intermediate velocity regime is characterized by the possibility of stick-slip motion whenever dF/dV has a negative slope [19,30]. Finally, for very low velocities, the motion is again Newtonian, even at high loads, but with a very high effective viscosity. This is the 'creep' regime where everything, even a crystalline solid, will flow like a viscous liquid — if measured over a sufficiently long time scale.

Just as in the case of other rheological or tribological constitutive equations, it is possible to construct other dynamic friction maps based on different variables such as $\sigma=F/A$, $\dot{\gamma}=V/D$ or $\mu=F/L$. However, we have chosen the variables of Figs. 4, 6 and Fig. 7 since these are usually the most easily accessible under experimental and engineering conditions. It is also worth noting that the friction coefficient, defined either by $\mu=F/L$ or by $\mu=dF/dL$, is unsuitable for many modern technological applications where friction forces exist under conditions of zero and even negative loads [31].

The key point here has been noted often over the years: whenever there exists an adhesive force between sliding surfaces (whether from reasons owing to capillary effects, electrostatic interactions, or the actual structure of the liquid film), substantial friction will usually be encountered even though the external normal load is negative. Equivalently, there exist numerous situations where the external load is substantial yet the friction force is negligible; one prominent example concerns the sliding of charged surfaces separated by double-layer electrostatic interactions in aqueous media.

Looking to the future, an important area for future study will involve extending the present results (which strictly apply to a micron-sized single asperity contact) to multiple non-coherent contacts as occurs between most 'real' sliding surfaces. In future work it will be important to similarly relate the overall friction force — an average over many asperity contacts — to experimentally-measurable local parameters.

6. Conclusion

Recent measurements of previously-inaccessible parameters have quantified the deviations from continuum behavior of ultra-thin films between two surfaces during frictional sliding. Two effects have been identified: (1) Over certain regimes of load and sliding velocity, the effective viscosity increases dramatically and is no longer Newtonian but depends on the shear rate according to the law $\eta_{\text{eff}} \propto \dot{\gamma}^{-n}$, where n varies between $-1/2$ and -1.0. This regime occurs between the upper and lower critical velocities. (2) Over a different regime, liquid-to-solid transitions can occur, where the local film structure changes abruptly as do the local tribological properties. The important tribological parameters (which are not the same as the Stribeck ones) are the velocity V, the load L, which determines D and hence the shear rate, and the molecular structure of the liquid (rather than the bulk viscosity), and also the surface lattice structure. Based on these new results, we have re-assessed the validity of current presentations of friction processes and proposed new constitutive relations and friction force phase diagrams that are formulated in terms of readily accessible or measurable parameters.

Acknowledgements

This work was supported by grants from the Exxon Research and Engineering Corporation. In addition, at the University of California, we acknowledge the Department of Energy (DOE) under grant DE-FG03-87ER45331 and the Ministerio de Educación y Ciencia (SPAIN) under FPI grant EX92-51359034. At the University of Illinois, we acknowledge the U.S. Air Force (AFOSR-URI-F49620-93-1-02-41) and the National Science Foundation (Tribology Program).

References

[1] M.L. Williams, R.F. Landel and J.D. Ferry, *J. Am. Chem. Soc., 77* (1955) 3701.
[2] J.D. Ferry, *Viscoelastic Properties of Polymers*, Wiley, New York, 3rd edn., 1980.
[3] K.C. Ludema and D. Tabor, *Wear, 9* (1966) 329.
[4] H. Yoshizawa, Y.L. Chen and J.N. Israelachvili, *J. Phys. Chem., 97* (1993) 4129.
[5] H. Yoshizawa, P. McGuiggan and J.N. Israelachvili, *Science, 259* (1993) 1305.
[6] Y. Liu, T. Wu and D.F. Evans, *Langmuir, 10* (1994) 2241.
[7] J. Van Alsten and S. Granick, *Phys. Rev. Lett., 61* (1988) 2570.
[8] S. Granick, *Science, 253* (1991) 1374.
[9] G. Carson, H.-W. Hu and S. Granick, *Tribology Transactions, 35* (1992) 405.
[10] M.L. Gee, P.M. McGuiggan, J.N. Israelachvili and A. Homola, *J. Chem. Phys., 93* (1990) 1895.
[11] G. Reiter, A.L. Demirel and S. Granick, *Science, 263* (1994) 1741.
[12] B. Bhushan, J.N. Israelachvili and U. Landman, *Nature, 374* (1995) 607.

[13] A.M. Homola, J.N. Israelachvili, M.L. Gee and P.M. McGuiggan, *ASME J. Tribology, 111* (1989) 675.
[14] P.A. Thompson, G.S. Grest and M.O. Robbins, *Phys. Rev. Lett., 68* (1992) 3448.
[15] P.A. Thompson, M.O. Robbins and G.S. Grest, *Isr. J. Chem., 35* (1995) 93.
[16] M. Schoen, S. Hess, and D.J. Diestler, *Phys. Rev. E, 52* (1995) 2587.
[17] J.N. Israelachvili, *Intermolecular and Surface Forces*, Academic Press, New York, 1992.
[18] A. Dhinojwala, L. Cai and S. Granick, *Langmuir, 12* (1996) 4537.
[19] J. Halling, *Principles of Tribology*, MacMillan, London, 1975.
[20] M. Urbakh, L. Daikhin and J. Klafter, *Phys. Rev. E, 51* (1995) 2137.
[21] Y. Rabin and I. Hersht, *Physica. A, 200* (1993) 708.
[22] G. Luengo, F.-J. Schmitt, and J.N. Israelachvili, *Macromolecules*, in press.
[23] S. Chynoweth, R.C. Coy, Y. Michopoulos and L.E. Scoles, *Synopsis Int. Tribology Conf.*, Yokohama, 1995.
[24] F.W. Smith, *Wear, 2* (1959) 250.
[25] S. Bair and W.O. Winer, *J. Tribology, 114* (1992) 1.
[26] E. Högland and B.O. Jacobson, *J. Tribology, 108* (1986) 571.
[27] C.R. Evans and K.L. Johnson, *Proc. Inst. Mech. Eng., 200* (1986) 303.
[28] A.C. Pipkin, *Lectures in Viscoelastic Theory* Springer–Verlag, New York, 1972.
[29] P. Panizza, P. Archambault and D. Roux, *J. Phys. II France, 5* (1995) 303.
[30] I.L. Singer and H.M. Pollock (eds.), *Fundamentals of Friction: Macroscopic and Microscopic Processes*, Kluwer, Dordrecht, 1991.
[31] J.N. Israelachvili, *Fundamentals of Friction: Macroscopic and Microscopic Processes*, Kluwer, Dordrecht, 1991.